JACS
JOURNAL OF THE AMERICAN CHEMICAL SOCIETY
Communication
pubs.acs.org/JACS

Water Oxidation by a Nickel-Glycine Catalyst

Dong Wang, Giovanna Ghirlanda, and James P. Allen*

Department of Chemistry and Biochemistry, Arizona State University, Tempe, Arizona 85287-1604, United States

Supporting Information

ABSTRACT: The utilization of solar energy requires an efficient means for its storage as chemical energy. In bioinspired artificial photosynthesis, light energy can be used to drive water oxidation, but catalysts that produce molecular oxygen from water are needed to avoid excessive driving potentials. In this paper, we demonstrate the utility of a novel complex utilizing earth-abundant Ni in combination with glycine as an efficient catalyst with a modest overpotential of 0.475 ± 0.005 V at a current density of 1 mA/cm^2 at pH 11. Catalysis requires the presence of the amine moiety with the glycine most likely coordinating the Ni in a 4:1 molar ratio. The production of molecular oxygen at a high potential is verified by measurement of the change in oxygen concentration, yielding a Faradaic efficiency of 60 ± 5%. The catalytic species is most likely a heterogeneous Ni-hydroxide formed by electrochemical oxidation. This Ni species can achieve a current density of 4 mA/cm^2 that persists for at least 10 h. Based upon the observed pH dependence of the current amplitude and oxidation/reduction peaks, the catalytic mechanism is an electron−proton coupled process.

While solar energy is an attractive option as a sustainable resource, the efficient conversion of solar energy into chemical fuels remains a challenge, with the natural diurnal cycle requiring a cost-effective, long-term storage mechanism.[1−5] One means for storage is using solar energy to generate hydrogen gas and molecular oxygen. However, current technologies are energetically inefficient due to the large overpotential associated with the electrolysis process. Consequently electrolytic water oxidation has a high energetic cost. Therefore, the development of efficient catalysts for the oxidation of water would greatly enhance the commercial viability of solar energy. In photosynthesis, water oxidation is performed by the Mn_4Ca cluster of the pigment−protein complex, photosystem II.[6] The efficiency and reproducibility of the catalytic mechanism is achieved by the accumulation of four charge equivalents at the Mn_4Ca cluster in a mechanism that is coupled with the transfer of four protons until the oxidation of water can occur. Progress in synthesizing water-oxidation catalysts has been made through the use of transition metals that can undergo multiple oxidation/reduction states. Research has been centered largely on metals such as ruthenium or iridium, but the operating conditions are often harsh, for example requiring acidic solutions, and the use of such precious metals is costly and not sustainable.[1,5,7−9] However, the use of a tetraGly peptide with copper was shown to enhance the catalytic properties of copper under benign conditions.[10]

To develop a low-cost, sustainable water-oxidizing catalyst, we have focused on the use of the earth-abundant metal nickel in the presence of amino acids. The electrochemical properties of Ni in the presence of glycine (Gly) were characterized by cyclic voltammetry (CV). In a 1 mM Ni solution in the absence of Gly, the measured current was relatively featureless and remained below 20 μA as the applied potential was increased from 0.2 to 1.45 V (Figure 1a). However, the addition of Gly resulted in a significant increase in the current to a measured value of 300 μA at 1.33 V for 4 mM Gly, corresponding to a current density of 4.2 mA/cm^2 (Figure 1b). With a fixed Ni:Gly molar ratio of 1:4, the amplitude of the current was directly proportional to the concentration of the catalyst up to 1 mM

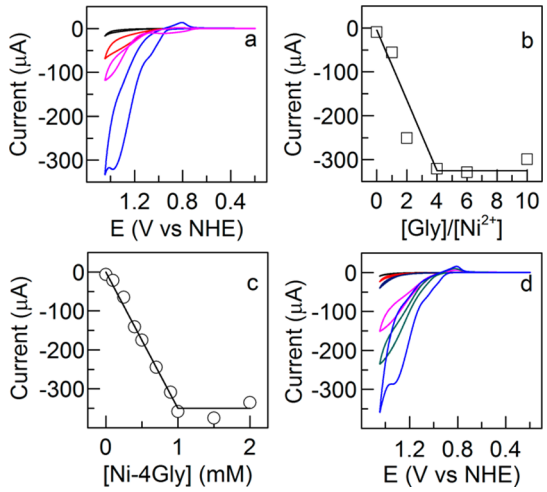

Figure 1. Electrochemical measurements of Ni(II) in a phosphate buffer at pH 11. (a) CVs measured using a glassy carbon working electrode with the potential swept from 0.20 to 1.45 V on a normal hydrogen scale (NHE). The CVs are relatively featureless with small currents for 1 mM Ni(II) alone (black), with an increase for 1 mM Gly (red) or 1 mM tetraGly peptide (pink), and a maximal current at a concentration of 4 mM Gly (blue). (b) The current for different amounts of Gly at 1 mM Ni at 1.38 V, showing a maximum at a 4:1 Gly:Ni molar ratio. (c) The current for different amounts of Ni-4Gly at 1.33 V, showing a maximum at a concentration of 1 mM Ni/4 mM Gly. (d) CVs have large currents for Ni(II) with amino acids, including glycine (blue), alanine (green), and glutamine (pink), and small currents for molecules with different substituents, including acetate (black), pyridine (red), and *N*-acetylglycine (dark blue).

Received: April 29, 2014
Published: July 3, 2014

Ni(II) after which the current was independent of the concentration, showing that the CV response is due to the Ni-4Gly system (Figure 1c). The stoichiometry was also tested by addition of a tetraGly peptide to Ni, which yielded a maximum current of 100 μA at 1.33 V for a Ni:tetraGly molar ratio of 1:1 (Figure 1a). Thus, these data are consistent with a stoichiometry of four Gly for every Ni yielding the maximum response.

The well-defined 1:4 ratio of Ni to Gly suggests that substituents of Gly serve as metal ligands. When amino acids other than Gly were added, such as alanine and glutamine, the CV response had an enhanced current at 1.33 V, showing that the side chain does not play a critical role (Figure 1d). However, only small currents of less than 40 μA were observed for other additives such as acetate, pyridine, and *N*-acetylglycine, which has a secondary amide and an acetyl substituent rather than the NH_2 of Gly. Together, these results demonstrate the involvement of the amine of glycine as playing a crucial role in the catalysis.

The catalytic enhancement of Ni with a tetraGly peptide is consistent with a previous report of water oxidation for Cu with a tetraGly peptide.[10] For the tetraGly peptide, the amines have been modeled as coordinating Cu(II) based upon infrared and electron paramagnetic resonance spectroscopies.[11,12] Coordination by four in-plane nitrogen atoms, from one primary amine and three secondary amides, and two out-of-plane oxygen atoms, from the carboxyl terminus and a bound water molecule, is found in the three-dimensional structure of Cu(II) bound to a tetraGly peptide.[10] Coordination by the amines to Ni is also suggested by the presence of three nitrogen ligands to Ni(II) in the structure of bis(glycylglyconato)nickelate(II).[13] Thus, for Ni-4Gly, the metal is most likely coordinated by four amines. For catalysis, only one primary amine is required based upon the current enhancement for the tetraGly peptide with Ni (Figure 1a).

The evolution of molecular oxygen as a product of the catalytic reaction was monitored by measuring the concentration of dissolved oxygen using a fluorescence-based oxygen sensor under controlled potential electrolysis. For the Ni-4Gly system, the oxygen concentration was constant with no applied potential but the change to a 1.33 V potential resulted in an increase in the oxygen concentration (Figure 2). After a short delay, presumably due to the time required for diffusion of oxygen from the electrode to the sensor, the oxygen concentration is observed to undergo a rapid increase. Based upon the initial rate, a Faradaic efficiency of 60 ± 5% is obtained when averaging three independent measurements, assuming the release of one oxygen molecule for every four electrons. The efficiency is less than unity most likely due to the formation of the catalytic species. These results demonstrate that the enhanced current at high potentials is associated with the production of molecular oxygen by the catalytic hydrolysis of water.

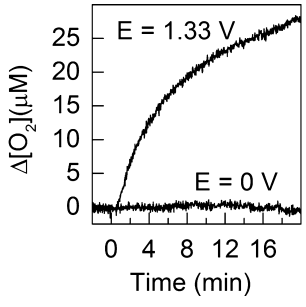

Figure 2. Time dependence of O_2 concentration change showing oxygen production for a Ni-4Gly solution when the potential is poised at 1.33 V compared to no applied potential. The initial rate of 4 μM/min yields a Faradaic efficiency of 61%. The sample contained 1 mM Ni and 4 mM Gly in phosphate buffer at pH 11.

The voltammograms have both an oxidative and reductive peak (Figure 3a). The reductive peak was observed on the cathodic scan as a broad feature at 0.78 V that increased in amplitude upon multiple scans. The oxidative peak was not initially evident but built up during subsequent scans as a sharp prefeature near 0.90 V suggesting the formation of the catalyst on the electrode. To test this possibility, 45 successive CV sweeps were performed in a solution containing both Ni and Gly. Then, the glassy carbon electrode was removed from the solution, lightly rinsed, and placed into a solution containing only 250 mM sodium phosphate without Ni or Gly. The resulting CV showed nearly the same current response as observed when the electrode was in the Ni-4Gly solution, with an enhanced current at 1.33 V of 170 μA (Figure 3b).

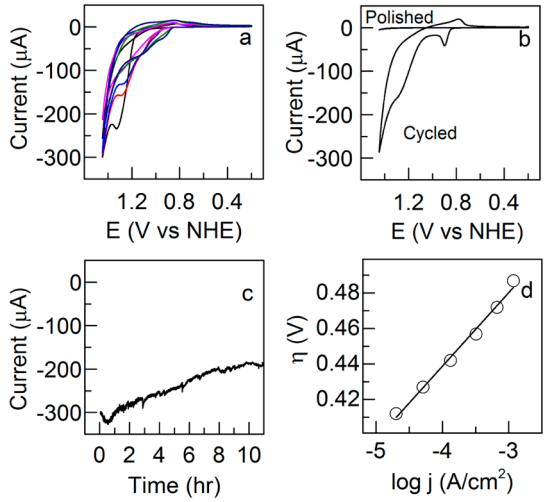

Figure 3. Electrochemical response of Ni-4Gly under different experimental conditions. (a) Forty-five consecutive scans were performed of an aqueous 1 mM Ni-4Gly solution in 250 mM phosphate buffer, pH 11, scan rate = 10 mV/s (Cycle 1 (black), 2 (red), 3 (light blue), 15 (pink), 30 (green) and 45 (dark blue)). (b) After 45 scans, a rinsed electrode in buffer alone shows the same features as seen in the Ni-4Gly solution; however no signals are present after polishing. (c) The measured current is very stable for 10 h at a fixed applied potential of 1.33 V. (d) The overpotential, η, which is the applied potential minus the thermodynamic potential of 0.575 V for water at pH 11, has a linear dependence on the current density, j, with a fitted slope of 0.04 V/decade and overpotential of 0.480 V.

Both the oxidation and reduction peaks at 0.78 and 0.90 V are present in the initial sweep of the rinsed electrodes in contrast to the observation of increases using polished electrodes in the Ni-4Gly solution. These results show that the CV features arise due to the formation of a Ni film on the carbon electrode. In solutions without Gly a film formed but at a much slower rate. When the electrode was prepared with 45 sweeps and then placed into a fresh Ni-4Gly solution, the current was very stable upon subsequent sweeps. The catalytic species was electrochemically deposited on the electrode as a film that is 0.7 μm thick after 45 sweeps (Figure S1). When the

dx.doi.org/10.1021/ja504282w | J. Am. Chem. Soc. 2014, 136, 10198−10201

potential was fixed at 1.33 V, the catalytic conditions were found to be very stable for several hours, retaining at least 60% of the maximum value for over 10 h (Figure 3c).

The measurement of a large and stable current indicates that water oxidation proceeds efficiently with a small overpotential, which is the applied potential minus the thermodynamic potential for water oxidation. The overpotential was determined by analysis of a Tafel plot that predicts a linear dependence of the overpotential on the current density. To minimize any contribution of forming the catalytic species, these measurements were performed using an electrode placed into buffer after 45 sweeps in a Ni-4Gly solution. A linear correlation was observed yielding an overpotential of 0.475 ± 0.005 V at a current density of 10^{-3} A/cm^2 based upon three independent measurements (Figure 3d).

The CV scans show pronounced changes as the pH was altered (Figure 4a). The amplitude of the current was negligible

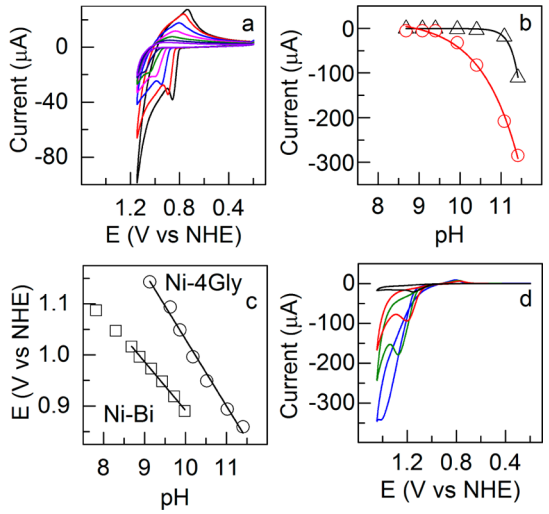

Figure 4. The pH dependence of the oxidation/reduction features. (a) The CV features of a Ni-film, produced by 45 consecutive scans, in 250 mM phosphate buffer shift to higher potentials as the pH is decreased (pH 11.40 (black), 11.02 (red), 10.52 (light blue), 10.18 (pink), 9.86 (green), 9.63 (dark blue), 9.13 (violet)). (b) pH dependence of the amplitude of the current at an applied voltage of 1.33 V (red circles) and 1.15 V (black triangles); the lines are a guide for the eye only. (c) The pH dependence of the position of the anodic prefeature (open circles) has a linear dependence on pH, with a best fit of −0.13 V/pH, compared to the dependence of −0.096 V/pH observed for Ni-borate (open squares) (ref 17). (d) Dependence of the CV on the concentration of phosphate, 0 mM (black), 50 mM (red), 100 mM (green), and 250 mM (blue), at fixed ionic strength for 1 mM Ni and 4 mM Gly.

below pH 9 and significantly increased above pH 9 (Figure 4b). The oxidation/reduction peaks near 0.78 and 0.90 V, at pH 11, are typical for Ni-oxide films and assigned to a one-electron, one-proton, oxidation/reduction couple, such as Ni(II)$(OH)_2$/Ni(III)O(OH).[16] The position of the anodic peak was found to systematically shift to higher potentials as the pH decreased (Figure 4c). A fit of the pH dependence for three independent measurements yielded a slope of −0.13 ± 0.01 V per pH, corresponding to the involvement of two protons.

The most likely catalytic mechanism for the Ni-4Gly system involves the generation of metal oxides in higher oxidation states, as has been found for other transition metals that facilitate water oxidation, such as copper, ruthenium, and iridium.[1,14−16] Energy-dispersive X-ray analysis showed the presence of Ni, P, and Na as the elemental components in addition to C, N, and O (Figure S2). Using X-ray photoelectron spectroscopy, the film was identified as containing Ni(II)−OH and PO_4^{3-} (Figure S3). Based upon the proposed mechanisms for other metal oxides,[1,7] a probable scheme includes a Ni(II)-hydroxide species binding a water molecule, being oxidized to Ni(IV), followed by the release of molecular oxygen and recovery to the divalent state of Ni in a proton-coupled process. These proton-coupled mechanisms are consistent with the pH dependence for the catalytic response.

In addition to Gly, the solutions for the CV measurements include 250 mM sodium phosphate. To investigate the contribution of phosphate, the CV measurements were performed for varying concentrations of sodium phosphate while keeping the ionic strength constant with the appropriate substitution of sodium perchlorate (Figure 4d). Increasing the sodium phosphate concentration resulted in a current response increase until a maximum was reached for a phosphate concentration of 250 mM. Notably, in the absence of phosphate, no enhancement of the current above 1.3 V was observed, but the voltammogram showed both the oxidation and reduction peaks, indicating that the Ni oxidation and reduction reactions occur despite the lack of water oxidation. Thus, phosphate is required for water oxidation, mostly likely serving as a proton acceptor.

Previously, Ni has been shown to serve as a water-oxidation catalyst in the presence of borate.[17−19] Compared to the Ni-4Gly catalyst, Ni-borate shares some characteristics such as a modest overpotential of 0.425 V compared to 0.475 V for Ni-4Gly, and the evolution of the oxidation/reduction peaks due to the formation of a Ni-oxide film. Also, in both cases a proton acceptor, phosphate or borate, is required. However, Ni-borate has the clear differences of the oxidation/reduction peaks being at lower potentials with a weaker pH dependence of the peak position (Figure 4), which has been interpreted as arising from a mechanism involving the coupled transfer of two electrons and three protons and the reversible dissociation of borate involving a dimer state of Ni.[17−21]

In summary, our results demonstrate the utility of a Ni-4Gly catalyst for the oxidation of water. This system has a modest overpotential of 0.475 V, is stable for prolonged periods of at least 10 h, and can achieve an activity of 4 mA/cm^2. This activity occurs under benign conditions in an aqueous solution using inexpensive materials. The catalysis of water oxidation is observed not only for Gly but also other amino acids and the tetraGly peptide providing the possibility of incorporating the catalyst into a peptide design that is attached to an electrode as part of a bioinspired solar cell. The presence of primary amines and phosphate is key to the formation of the heterogeneous, catalytically active Ni-hydroxide species, suggesting a new avenue for the development of water oxidation catalysts.

■ ASSOCIATED CONTENT

Supporting Information

Experimental details are available in the Supporting Information. This material is available free of charge via the Internet at http://pubs.acs.org.

■ AUTHOR INFORMATION

Corresponding Author

*E-mail: JAllen@asu.edu.

Notes

The authors declare no competing financial interest.

■ ACKNOWLEDGMENTS

This material is based upon work supported as part of the Center for Bio-Inspired Solar Fuel Production, an EFRC funded by the U.S. DOE, Office of Science, Office of Basic Energy Science Number DE-SC0001016. We thank the LeRoy Eyring Center for Solid State Science at ASU for SEM-EDX measurements and the Laboratory for Electron Spectroscopy and Surface Analysis at University of Arizona for XPS measurements.

■ REFERENCES

(1) Lewis, N. S.; Nocera, D. G. *Proc. Natl. Acad. Sci. U.S.A.* **2006**, *43*, 15729−15735.
(2) Youngblood, W. J.; Lee, S.-H. A.; Maeda, K.; Mallouk, T. E. *Acc. Chem. Res.* **2009**, *42*, 1966−1973.
(3) Cook, T. R.; Dogutan, D. K.; Reece, S. Y.; Surendranath, Y.; Teets, T. S.; Nocera, D. G. *Chem. Rev.* **2010**, *110*, 6474−6502.
(4) Walter, M. G.; Warren, E. L.; McKone, J. R.; Boettcher, S. W.; Mi, Q.; Santori, E. A.; Lewis, N. S. *Chem. Rev.* **2010**, *110*, 6446−6473.
(5) Gust, D.; Moore, T. A.; Moore, A. L. *Faraday Discuss.* **2012**, *155*, 9−26.
(6) Wydrzynski, T. J., Satoh, K., Eds. *Photosystem II*; Springer: Dordrecht, 2005.
(7) Cao, R.; Lai, W.; Du, P. *Energy Environ. Sci.* **2012**, *5*, 8134−8157.
(8) Fukuzumi, S.; Hong, D. *Eur. J. Inorg. Chem.* **2014**, *2014*, 645−659.
(9) Hong, D.; Yamada, Y.; Nagatomi, T.; Takai, Y.; Fukuzumi, S. *J. Am. Chem. Soc.* **2012**, *134*, 19572−19575.
(10) Zhang, M. T.; Chen, Z.; Kang, P.; Meyer, T. J. *J. Am. Chem. Soc.* **2013**, *135*, 2048−2051.
(11) Kim, M. K.; Martell, A. E. *J. Am. Chem. Soc.* **1966**, *88*, 914−918.
(12) Nagy, N. V.; Szabo-Planka, T.; Rockenbauer, A.; Peintler, G.; Nagypal, I.; Korecz, L. *J. Am. Chem. Soc.* **2003**, *125*, 5227−5235.
(13) Freeman, H. C.; Guss, J. M. *Acta Crystallogr.* **1978**, *B34*, 2451−2458.
(14) Crabtree, R. H. *Chem. Rev.* **2012**, *112*, 1536−1554.
(15) Artero, V.; Fontecave, M. *Chem. Soc. Rev.* **2013**, *42*, 2338−2356.
(16) Doyle, R. L.; Godwin, I. J.; Brandon, M. P.; Lyons, M. E. G. *Phys. Chem. Chem. Phys.* **2013**, *15*, 13737−13783.
(17) Dinca, M.; Surendranath, Y.; Nocera, D. G. *Proc. Natl. Acad. Sci. U.S.A.* **2010**, *107*, 10337−10341.
(18) Bediako, D. K.; Lassalle-Kaiser, B.; Surendranath, Y.; Yano, J.; Yachandra, V. K.; Nocera, D. G. *J. Am. Chem. Soc.* **2012**, *134*, 6801−6809.
(19) Bediako, D. K.; Surendranath, Y.; Nocera, D. G. *J. Am. Chem. Soc.* **2013**, *135*, 3662−3674.
(20) Risch, M.; Klingan, K.; Heidkamp, J.; Ehrenberg, D.; Chernev, P.; Zaharieva, I.; Dau, H. *Chem. Commun.* **2011**, *47*, 11912−11914.
(21) Singh, A.; Chang, S. L. Y.; Hocking, R. K.; Bach, U.; Spicca, L. *Energy Environ. Sci.* **2013**, *6*, 579−586.